HAL
archives-ouvertes.fr

Radiometric Attenuation for Beacon Calibration: a Preliminary Analysis on Accuracy and Reliability

V. Mattioli, A.V. Bosisio, X. Boulanger, L. Castanet

▶ **To cite this version:**

V. Mattioli, A.V. Bosisio, X. Boulanger, L. Castanet. Radiometric Attenuation for Beacon Calibration: a Preliminary Analysis on Accuracy and Reliability. 8th European Conference on Antennas and Propagation (EUCAP 2014), Apr 2014, LA HAYE, Netherlands. pp.672 - 676, 2014, <10.1109/EuCAP.2014.6901849>. <hal-01058712>

HAL Id: hal-01058712

https://hal-onera.archives-ouvertes.fr/hal-01058712

Submitted on 8 Oct 2014

HAL is a multi-disciplinary open access archive for the deposit and dissemination of scientific research documents, whether they are published or not. The documents may come from teaching and research institutions in France or abroad, or from public or private research centers.

L'archive ouverte pluridisciplinaire **HAL**, est destinée au dépôt et à la diffusion de documents scientifiques de niveau recherche, publiés ou non, émanant des établissements d'enseignement et de recherche français ou étrangers, des laboratoires publics ou privés.

Radiometric Attenuation for Beacon Calibration: a Preliminary Analysis on Accuracy and Reliability

Vinia Mattioli[1], Ada Vittoria Bosisio[2], Xavier Boulanger[3], Laurent Castanet[3]
[1] HeSpace Operations GmbH, Darmstadt, Germany, Vinia.mattioli@ieee.org
[2] CNR/IEIIT, Milano, Italy, ada.bosisio@ieiit.cnr.it
[3] ONERA/DEMR; Toulouse, France, Xavier.Boulanger@onera.fr, Laurent.Castanet@onera.fr

***Abstract*— A microwave radiometer profiler is used to determine the no-attenuation level relative to which beacon atmospheric attenuation is measured. A technique that can be used for the discrimination of atmospheric conditions (clear-sky, cloudy, rainy) from the measured slant-path brightness temperatures is discussed, with the aim of improving the accuracy and the reliability of the radiometric correction.**

***Index Terms*—microwave radiometer, atmospheric attenuation, beacon calibration.**

I. INTRODUCTION

The availability of long operating satellites in the 20/30 GHz band offers the opportunity for investigating various aspects related to the channel characterization and its performances, such as uplink or downlink power control, site diversity, frequency diversity, and so on. Nowadays, new services should comply with specific requirements in terms of outage percentage and/or Quality of Service (QoS). Among other impairments, those due to strong rain events could affect dramatically the signal quality. In order to increase link availability, without limiting too much system capacity, Fade Mitigation Techniques (FMT) adapting the waveform in real time (ACM) or foreseen as planned act (VCM) are used and/or standardized. The identification and the optimization of the FMT strategy could rely on the channel characterization along concurrent Earth-to-satellite path.

During the last two decades, researchers have investigated the usefulness of concurrent and collocated radiometric measurements with beacon receivers to predict atmospheric attenuation along a satellite path [1-2]. Radiometers are employed to assess a reference level for the atmospheric attenuation experienced under clear-sky conditions towards the beacon level calibration, through the so-called bias removal procedure [3].

In order to provide meaningful statistics and time series, the ability to discriminate between different atmospheric conditions on the satellite link path is crucial. From radiometric measurements, an empirical real time criterion, the Sky Status Indicator (*SSI*), proved to be useful to discriminate among clear, cloudy and rainy conditions along the propagation path [4-5]. *SSI* issues from the ratio between the brightness temperature values measured in the band of interest and its identification capabilities were validated against rain gauge measurements [6]. In the present work, authors take advantage of one year of measurements collected from a beacon receiver of the satellite ASTRA 3B and from a collocated microwave radiometer at the ONERA's main building in Toulouse, France. Data observed between July 2012 and June 2013 are exploited to investigate the correlation between the received beacon signal (CPA) and the concurrent SSI values. By using the rain rate (*RR*) measurements of a collocated rain gauge, a statistical analysis that relies on the couples (*RR*, *SSI*) as given from their complementary cumulative distribution function (CCDF) has been performed. The goal was to single out the attenuation reference level for beacon measurement together with the estimate of the rain atmospheric attenuation during rain events. Finally, results were inspected through a careful check on single events.

II. MEASUREMENT DATABASE

A. Beacon Receiver

The beacon receiver deployed in ONERA, Toulouse (F), was initially designed to receive the 20.7 GHz beacon of Stentor. After the loss of the satellite, it was upgraded to receive the 19.7 GHz beacon of Eutelsat HotBird 6 [7-8]. Since March 2011, the beacon receiver is at the third stage of its upgrade by receiving the 20.2 GHz beacon of the ASTRA-3B satellite, along a propagation slant path at θ= 35.2°. The receiver is comprised of a Cassegrain parabolic antenna of 1.20 m. The RF chain is immediately located at the output of the antenna in order to avoid feeder loss. Two frequency down-conversions are performed, a first one from 20.2 GHz to 110 MHz and a second one from 110 MHz to 10 MHz. The first frequency conversion is made by an active receiving head that is composed of a low noise amplifier, a mixer and another amplifier. In order to eliminate spurious, the signal is band-pass filtered and then amplified. After being filtered once again (to eliminate amplifiers parasitic products), the second frequency conversion is made. Then, the re-amplified and filtered signal is processed by a DDS card.

B. Radiometric Unit

The ONERA radiometric unit deployed in Toulouse is a profiling radiometer TP/WVP-3000 developed by Radiometrics (USA) [9, 10]. It observes atmospheric

brightness temperatures in five frequency bands from 22 to 30 GHz, and in seven bands from 51 to 59 GHz. It also measures surface temperature, humidity, and pressure. The radiometer has automated elevation- scanning capability and the observation interval can be as short as several seconds. The instrument is collocated with the beacon receiver (1 m apart). In its current configuration, it continuously measures along a propagation slant path at θ= 35.2°, while performing tip curves every hour. An absolute calibration with liquid nitrogen is also performed every six months.

C. Pluviometer

The ONERA rain gauge deployed in Toulouse is a dual-chambered tipping bucket manufactured by FIEDLER, CZ, with a collecting area of 500 cm^2, 0.1 mm per pulse resolution and 0.015 mm accuracy. Rain rate measurements (RR, $mm \cdot h^{-1}$) were obtained according to the methodology described in [11].

III. THEORETICAL ASPECTS

A. Bias removal procedure

Because of Satellite EIRP variations, antenna mispointing, receiver RF chain variations, the link budget is not known accurately. It follows that beacon measurements are relative, instead of being absolute. the attenuation reference level is not constant and ancillary equipment is required to overcome this uncertainty. Radiometers are used to this purpose [3].

Based on the Radiative Transfer Equation and on the definition of the mean radiating temperature T_{mr} [12, 13], the relationship between the total atmospheric attenuation at frequency $f_{rad,i}$, $A_{rad}\left(f_{rad,i}\right)$, and the brightness temperature, $T_b\left(f_{rad,i}\right)$, is derived by using:

$$A_{rad}\left(f_{rad,i}\right) = 10\log_{10}\left(\frac{T_{mr} - T_c}{T_{mr} - T_b\left(f_{rad,i}\right)}\right) \quad (1)$$

where T_c is the temperature of the cosmic noise (usually T_c=2.7 K). T_{mr} temporal series were computed from collocated standard surface meteorological measurements according to:

$$T_{mr}(\theta, f) = d_0 + d_1 T_S + d_2 P_S + d_3 RH \quad (2)$$

where T_s, P_s, and RH are respectively the measurements of air temperature, pressure and relative humidity at the surface. Specific coefficients d_i were computed using regression analysis depending on frequency and elevation angle, as described in [14]. With this relation, T_{mr} can be estimated with approximately 1% rmse for a wide range of locations and sky conditions [14].

Then, the radiometer attenuation at the beacon frequency (here 20.2 GHz) can be computed through:

$$A_{rad}(20.2) = a_0 + \sum_{f_{rad,i}} a_i A_{rad}\left(f_{rad,i}\right) \quad (3)$$

where $f_{rad,i}$ are specific selected radiometric frequencies [10]. The attenuation value retrieved from the radiometer allows the extraction of reference "0-dB level" templates A_{0dB} during not rainy conditions:

$$A_{0dB}(t) = \langle S(t) \rangle + A_{rad}(t) \quad (4)$$

where $<S(t)>$ is the filtered beacon signal (negative by reference). rainy conditions, since the information from the microwave radiometer cannot be used reliably, the A_{0dB} Hence , A_{0dB} is reconstructed through linear interpolation observing the period before and after the event. The main steps of the data processing methodology are the following:

- Measured Instrumental Data (MID raw data collected by each instrument) are merged into one Raw Propagation Data (RPD) file with common time reference and standard validity flags.
- RPD files are analysed to remove long-term variations due to both antenna mispointing and temperature dependence. Validity flags are inspected and changed, if necessary. Then, the results are stored into Intermediate Propagation Data (IPD) files.
- Finally, Validated Time Series (VTS) of copolar attenuation (CPA) are generated according to:

$$CPA(t) = S(t) - A_{0dB}(t) \quad (5)$$

At the end of the process, the copolar level gives the atmospheric attenuation contribution, that is the reference clear-sky attenuation in "rain-free" conditions (i.e. non scattering phenomena), the beacon attenuation in periods of scattering conditions and the scintillations measured by the beacon receiver during the overall time period. Satellite contribution are removed and *CPA* expresses the fading solely due to the atmosphere.

B. SSI threshold

SSI is an index based on radiometric observations and it computed as the ratio between two frequency lines in the 20/30 GHz band. Its value issues from a clear sky analysis of the propagation path that aims at removing the dry contribution of the gaseous phase of the atmosphere [4-6]. In our case, *SSI* is computed according to:

$$SSI = \frac{T_b(30) - c_0}{T_b(23.8)} \quad (6)$$

where the coefficient c_0=9.8 K. Details on its computation are given in [5-6]. *SSI* values were computed and associated to the corresponding radiometric measurements.

As shown in Section IV, having set a proper boundary threshold value to discriminate between cloudy and rainy conditions, *SSI* can be used to identify rainy periods. Hence, the reference 0-dB level A_{0dB} can be computed according to the methodology described in Section III.A.

IV. STATISTICAL ANALYSIS

The relationship between the observed precipitation rain rate RR, the computed *SSI* values and the received beacon attenuation *CPA* is analyzed through a statistical approach based on the corresponding complementary cumulative distribution functions CCDF of these quantities.

The basic idea is to single out the *SSI* value that corresponds to an observed precipitation rate and to use this threshold value to identify in the received beacon signal the onset of a rain event. The choice of the *SSI* threshold level is driven by the probability level at which occurs a specific *RR* value in its yearly CCDF.

Fig. 1 (top) shows the CCDFs of the *RR* measured during the year, whereas the bottom panel gives the *SSI* CCDF. both relative to the year of observation in Toulouse. Let $\boldsymbol{r}=\{RR_i\}$ be the vector of the precipitation rate values and $\boldsymbol{p}_r\{P_{RRi}\}$ the vector of the corresponding probability value. The element of $\boldsymbol{p}_r$ are used as input in the *SSI* CCDF to resort the vector $\boldsymbol{s}=\{SSI_i\}$ of the *SSI* values that occur at the probability level of RR. At the end of this step, one obtains a couple of values (RR_i, SSI_i) occurring at the same probability level. Fig.2 shows the result of this selection process as a scatter diagram of SSI versus *RR*. The diagram highlights the range of the lower values of both *RR* and *SSI* since it aims at investigating suitable *SSI* values that can be used as thresholds (to identify suitable radiometer data for the extraction of the 0-dB level). Few couples were identified: *SSI* ≤0.73 for *RR*≤0.25 mm·h^{-1}; *SSI* ≤0.84 for RR≤0.5 mm·h^{-1}; and *SSI* ≤0.87 for *RR* ≤0.8 mm·h^{-1}. It can be noticed that the value of 0.87 was also identified in [14] through a different approach. The *RR* intensities were set heuristically at 0.25, 0.5 and 0.8 mm-hr-^{1}. The first value is intended to identify very light/light rain event, whereas the remaining two are intended as the lower intensity values of precipitation events. It is to be reminded that the final goal is to discriminate the presence of rain along the path, where the atmosphere structure is far from being homogeneous and uniform. That is to say that the choice of the *RR* value, which leads to the SSI threshold value definition, is still an open question.

The following considerations can be made:

(a) the *SSI* vs RR curve in Fig.2 shows how *SSI* saturates as *RR* increases. This is an expected behavior, nevertheless it can be noticed that the slope of the curve changes near *SSI*=0.85 and *SSI*=0.95 behavior. the *SSI* vs *RR* curve in Fig.2 shows how *SSI* saturates as *RR* increases. This is an expected behavior, nevertheless it can be noticed that the slope of the curve changes near *SSI*=0.85 and *SSI*=0.95. One crucial point of this process, i.e. the influence of the *RR* bin size in the *SSI* identification, needs further investigation. This is especially true when working with low *RR* intensities values collected by rain gauges.

(b) selecting the proper threshold necessarily involves accounting for the associated error detection probability and balancing according to which condition is important to appropriately respond. The Bayes criterion is an approach suitable for such cases and it will be further investigated. For instance, a suitable SSI threshold could choose between either a more conservative approach that provides an accurate selection of clear and cloudy conditions -lowest value of *SSI*- or a slightly relaxed approach that allows the use of radiometer

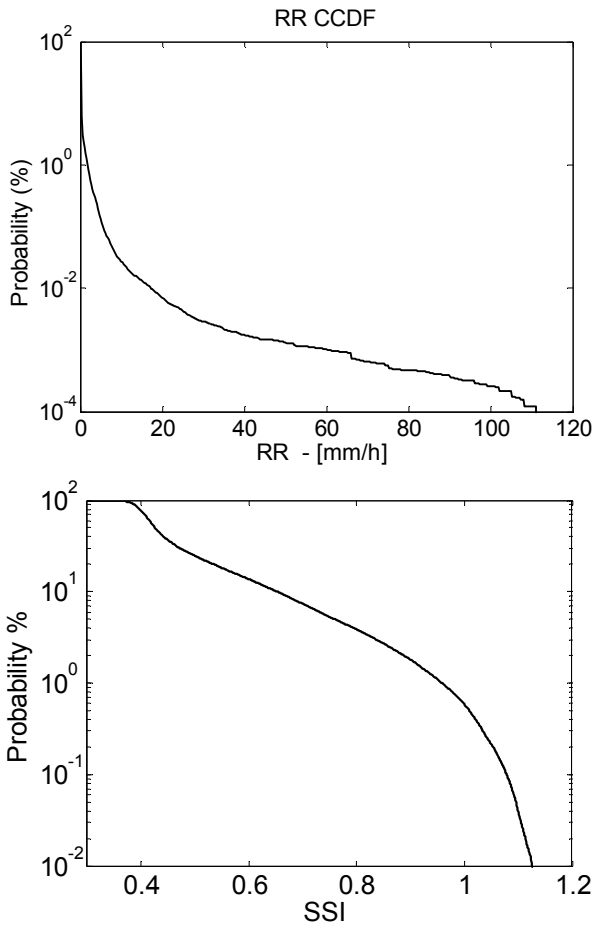

Fig. 1. (top) CCDF of RR derived from the pluviometer measurements collected at Onera between July 2012 and June 2013. (Bottom) CCDF od SSI derived from the ground-based microwave radiometer.

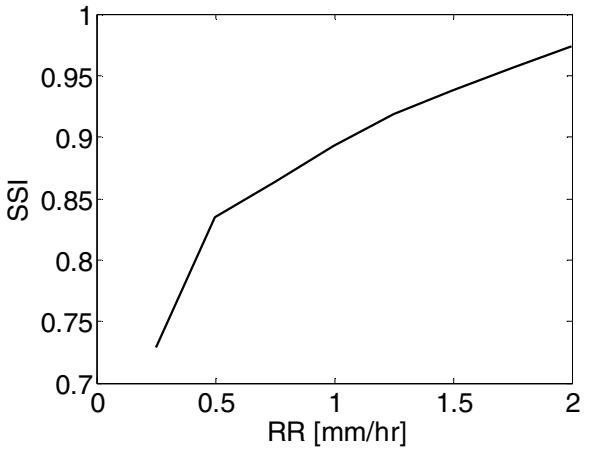

Fig. 2. Scatter diagram of SSI versus RR chosen at the same probability level

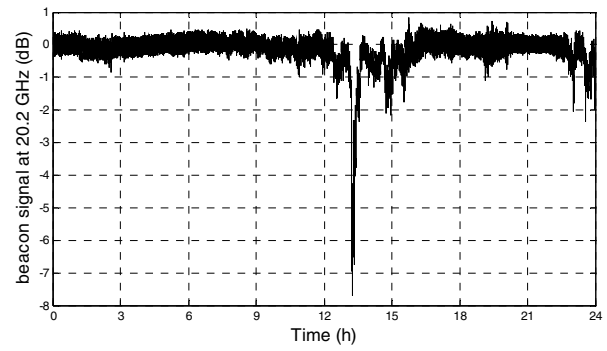

(a)

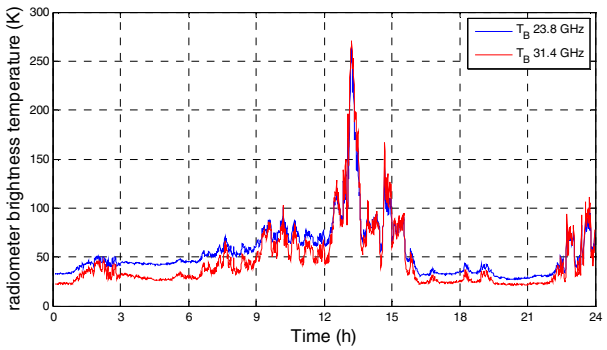

(b)

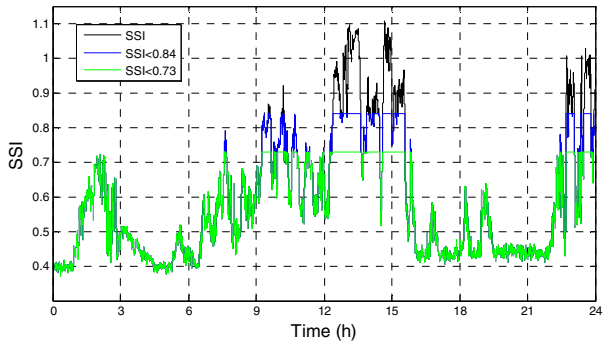

(c)

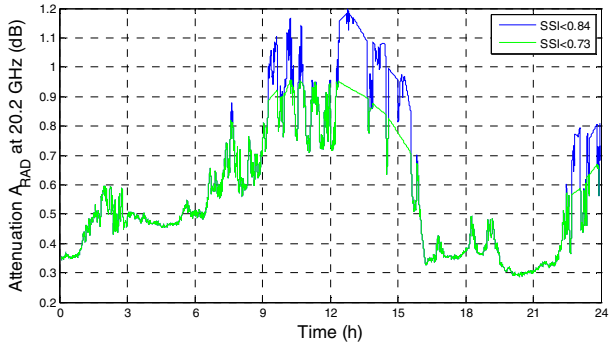

(d)

Fig. 3. (a) Beacon signal received on December 7, 2012. (b) Measured radiometric T_B's at 23.8 and 31.4; (c) SSI values and (d) corresponding atenuation A_{rad} at 20.2 GHz.

larger portion of the time (within the starting point of the rainy event)- highest value of *SSI*. At present, the second approach was preferred; therefore, *SSI* statistics concurring with the beginning of rain were investigated.

The next step in this statistical approach is to obtain the vector $\boldsymbol{c}$= {CPA_i} to relate *SSI* to the beacon attenuation. To do this, the rain contribution to the atmospheric attenuation has to be removed, as described in Section V.

V. Event-based analysis

The results of the approach described in Section IV were also analyzed through a event-based analysis.

An example is shown in Figs. 3-5, applied to the beacon signal received on December 7, 2012 (Fig. 3a). Measured radiometric T_B's are given in Fig. 3b, while the corresponding *SSI* values are shown in Fig. 3c. According to the *SSI* threshold method, the radiometric-retrieved attenuation (eq. 3) is discarded for the period in which the concurrent *SSI* value is greater than the threshold (Fig. 3d), as it cannot be used to compute the reference level. Fig.4 shows the 0-dB level (eq. 4) that outcomes from the identification of rainy period by using *SSI*<0.84, in the top panel, and *SSI*<0.73, in the bottom panel. The computation of A_0 is here compared with the one that is obtained by visual inspection of the signal (here as the reference). Whether during rain-free periods the two approaches give similar results, differences emerge while raining. In particular, the SSI-selected time series shows a piece-wise linear with abrupt slope changes due to the linear interpolation (§IIIA). Possible countermeasures could be either to low pass filter the *SSI* time series or the radiometric attenuation during rain. Both strategies will be investigated in the next future.

As final step, the *CPA* signal as in eq. (5) is computed by subtracting the retrieved attenuation from the beacon signal. Fig. 5 shows the beacon attenuation as result of the bias removal, by using *SSI*<0.73 (top panel) and *SSI*<0.84 (bottom panel).

Common practice considers using the "wet window" sensor installed on the radiometer to flag on radiometer data, but the procedure mainly relies on visual inspection of the time series. Problems arise since the wet window flag refers to in-situ values that may differ from slant-path observations along the line-of-sight beam. After strong rain events, drifts in the radiometer measurements may be present, which indicate residual humidity on the antenna radome that can be flagged through *SSI*. These are the reasons why an automatic methodology as the *SSI* index, which is based on the intrinsic quality of the measured brightness temperatures, represents a quite relevant tool.

VI. Conclusions

The use of SSI as a selection tool for the microwave measurements in the beacon bias removal procedure was analyzed considering different threshold values for *SSI*. The strategy that leads to the selection of the proper *SSI* values is based on the precipitation intensity associated to the rain

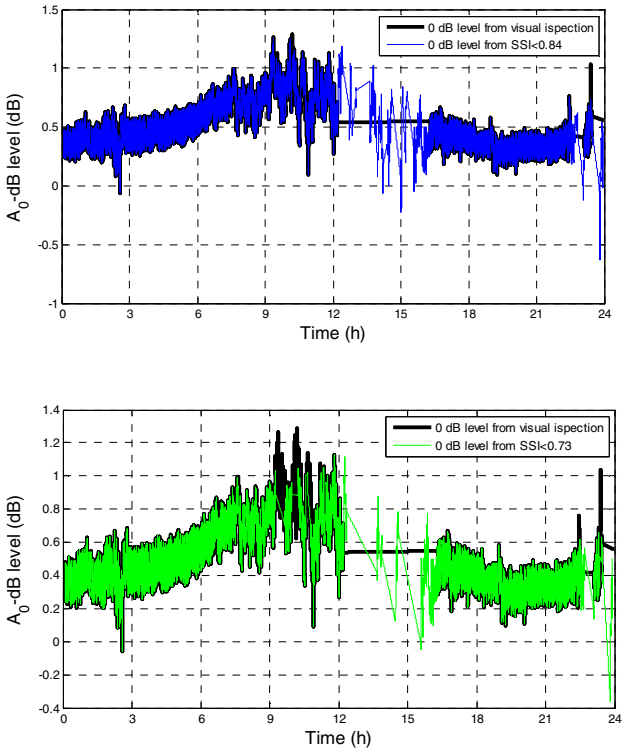

Fig. 4. A_0-dB level for the beacon measurements on December 7, 2012, using as threshold (top) SSI<0.87 and (bottom) SSI<0.73 as compared with CPA derived from visual inspection (black curve).

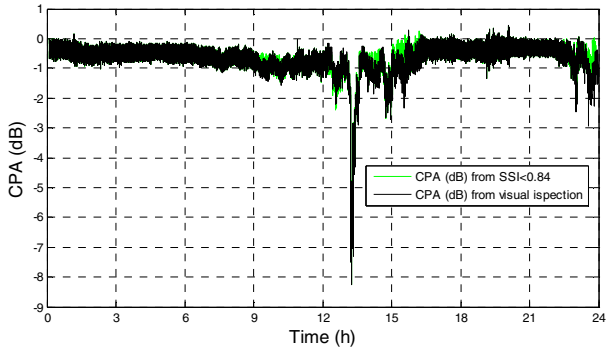

Fig 5. Beacon CPA (dB) on December 7, 2012 form SSI<0.73 as compared with CPA derived from visual inspection (black curve).

events the one want to discard towards 0-db level assessment. Here, the choice was driven by concurrent rain gage measurements, but refinements may be brought by additional ancillary measurements. The *CPA* extraction was described and tested against visual inspection on measurements collected on December 7, 2012. Although a larger analysis is necessary before reaching a conclusion, the optimal choice of *SSI* could profit of the associated attenuation uncertainty resulting by the analysis of its CCDF analysis, as suggested in Section IV.

REFERENCES

[1] Paraboni A., G. Masini, M. Mauri, R. Polonio and C. Riva, "Summary of propagation results obtained in 5 years of ITALSAT experiment in Milano", International Journal of Satellite Communications, VOL. 17, Issue 1, 1999, pp. 169-175.

[2] OPEX Second Workshop of Olympus Propagation Experimenters. Vol. 3: Reference book on Radiometry and Meteorological Measurements, 8-10 Nov, Noordwijk (NL), ESA WPP-083,1994.

[3] Mallet, C., J. Lavergnat, Beacon calibration with a multifrequency radiometer, Radio Science, Vol. 27, No.5, pp. 661-680, 1992.

[4] Bosisio A.V., Ciotti P., Fionda E., Martellucci A. (2013) - Preliminary Results on the Performance of an Indicator to Identify the Status of the Sky Along a Satellite Link by Means of Ground-Based Brightness Temperatures, 7th EUCAP, pp. 268-272, , Goteborg (SW), April 2013.

[5] Bosisio A.V., Fionda E., Basili P., Carlesimo G., Martellucci A- Identification of rainy periods from ground-based microwave radiometry, European Journal of Remote Sensing, Vol. 45, pp. 41-50. 2012a.

[6] Bosisio A.V., Ciotti P., Fionda E., Martellucci A. - A sky status indicator to detect rain-affected atmospheric thermal emissions observed at ground, IEEE Trans. GRS, Vol. 51, No. 9, pp. 4643-4649, 2013.

[7] Boulanger X., Carrie G., Casadebaig L., Gabard B. and Castanet L., "Statistics of Total Attenuation Measurements in Toulouse from the 19.7 GHz Beacon of Eutelsat Hotbird 6", ESA Workshop on radiowave propagation 2011, ESTEC, Noordwijk, The Netherlands, November 30 – December 2, 2011.

[8] Boulanger X., Nguyen H.J., Casadebaig L., Gabard B., Castanet L. : "Statistcs of total and rain attenuation measurements in Toulouse from the 20.2 GHz beacon of ASTRA-3B", Joint 19th Ka and Broadband Communications, Navigation and Earth Observation Conference – 31st AIAA International Communications Satellite System Conference (ICSSC), Firenze, September 2013.

[9] Solheim F., J. Godwin, E. Westwater, Y. Han, S. Keihm, K. Marsh and R. Ware, Radiometric Profiling of Temperature, Water Vapor, and Cloud Liquid Water using Various Inversion Methods, Rad. Sci., 33, pp. 393-404, 1998.

[10] Solheim, F., J. Godwin and R. Ware, Microwave Radiometer for Passively and Remotely Measuring Atmospheric Temperature, Water Vapor and Cloud Liquid Water Profiles, US Army White Sands Missile Range Final Report, 52 pp., 1996. [available at: http://radiometrics.com/data/uploads/2012/11/solheim_WSMR_96.pdf].

[11] Fiser O. et al., Meteorologiacal measurements, Chapter 3 in COSTIC0802 Handbook of Measurements.

[12] Ulaby F.T., R.K.Moore and A.K.Fung, Microwave Remote Sensing Active and Passive, Vol.1, Addison-Wesley, 288-302, 1981

[13] Mattioli, V. , F.S. Marzano, S. Crewell, G. Carrie, U. Löhnert, D. Cimini, E. Fionda, A. Martellucci, " Instruments, Data and Techniques for the Assessment of the Atmospheric Noise Emission in Satcom Ground Stations", Proc. of 6th European Conference on Antennas and Propagation (Eucap 2012), Prague, 26-30 March 2012.

[14] Mattioli V, 2013, "Definition of radiometric coefficients", Alphasat TDP5 GS G/T measurement campaign and IOT GS4-MWR, Graz, Austria, 20pp.

[15] Mattioli V., A. Graziani, P. Tortora, A. V. Bosisio, L. Castanet, "Analysis and improvements of methodologies for discriminating atmospheric conditions from radiometric brightness temperatures," Proc. of Antennas and Propagation (EuCAP), 2013 Page(s): 1392- 1396.